The relation of the atomic mass ratio and quartic anharmonicity in alkali metal hydrides

Minxuan Feng,[1, †] Xiaoying Wang,[1, †] Guimei Zhu,[2,*] Cheng He,[1]
Jun Sun,[1] Xiangdong Ding,[1] Junichiro Shiomi,[3] Yi Xia,[4] Baowen Li,[5] and Zhibin Gao[1, ‡]
[1]State Key Laboratory for Mechanical Behavior of Materials,
Xi'an Jiaotong University, Xi'an 710049, China
[2]School of Microelectronics, Southern University of Science and Technology, Shenzhen, 518055, China
[3] Department of Mechanical Engineering, The University of Tokyo, Tokyo 113-8656, Japan
[4] Department of Mechanical and Materials Engineering,
Portland State University, Portland, Oregon 97201, USA
[5]Department of Materials Science and Engineering,
Department of Physics. Southern University of Science and Technology, Shenzhen, 518055, PR China

† These authors contributed equally to this work.
[*] E-mail: zhugm@sustech.edu.cn
[‡] E-mail: zhibin.gao@xjtu.edu.cn

We find that XH material has strong phonon-phonon anharmonicity, which leads to a low κ_L. The energy of the system with atomic displacement following the transverse optical (TO) phonon mode can be fitted by a polynomial function, as depicted in Fig. S1. The atomic displacement pattern, which corresponds to the one displayed in the inset of Fig. S1, was achieved by moving all atoms of the system according to this specific vibration mode. In regards to the TO phonon mode, the vibrational direction of the X atom runs parallel to the H atom, albeit in the opposite direction (inset). When all atoms were moved along its eigenvector, the energy curve significantly deviated from the harmonic (i.e., second-order fitting) model.

To fit the energy curve as a function of displacement, we utilized the equation $y_i = a_i x^2 + b_i x^3 + c_i x^4$. The coefficients of a_i b_i c_i for five materials are given in TABLE SI. It seems that the quartic term is quite significant which is reflected by the amplitude of value c_i. Interestingly, as the atomic mass ratio increases, both the quadratic and quartic coefficients decrease. Additionally, the a_i and c_i coefficients exhibit similar fitting values, further suggesting the strong anharmonicity of XH materials [1, 2].

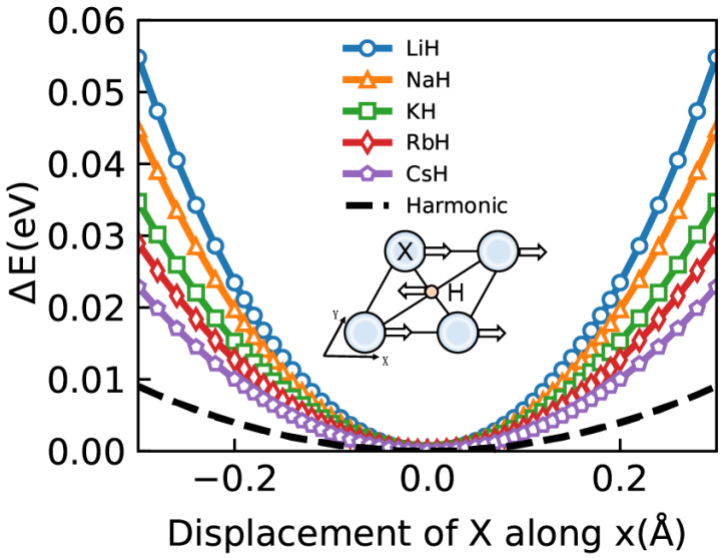

FIG. S1. The solid lines represent anharmonic frozen-phonon potential with polynomial fitting. $y_i = a_i x^2 + b_i x^3 + c_i x^4$, fitting data shown in TABLE SI. The dashed line represents harmonic approximation $\Delta E \propto x^2$. The inset shows the vibration direction of the lowest-energy TO_X phonon mode.

TABLE SI. The energy profile with atomic displacement following the transverse optical (TO) phonon mode can be fitted by a polynomial function as $y_i = a_i x^2 + b_i x^3 + c_i x^4$ in XH compounds (X = Li, Na, K, Rb, Cs).

XH	a_i	b_i	c_i
LiH	0.589	4.123×10^{-10}	0.450
NaH	0.489	5.068×10^{-5}	0.105
KH	0.378	-2.838×10^{-8}	0.0875
RbH	0.315	2.936×10^{-15}	0.0693
CsH	0.247	1.724×10^{-10}	0.0785

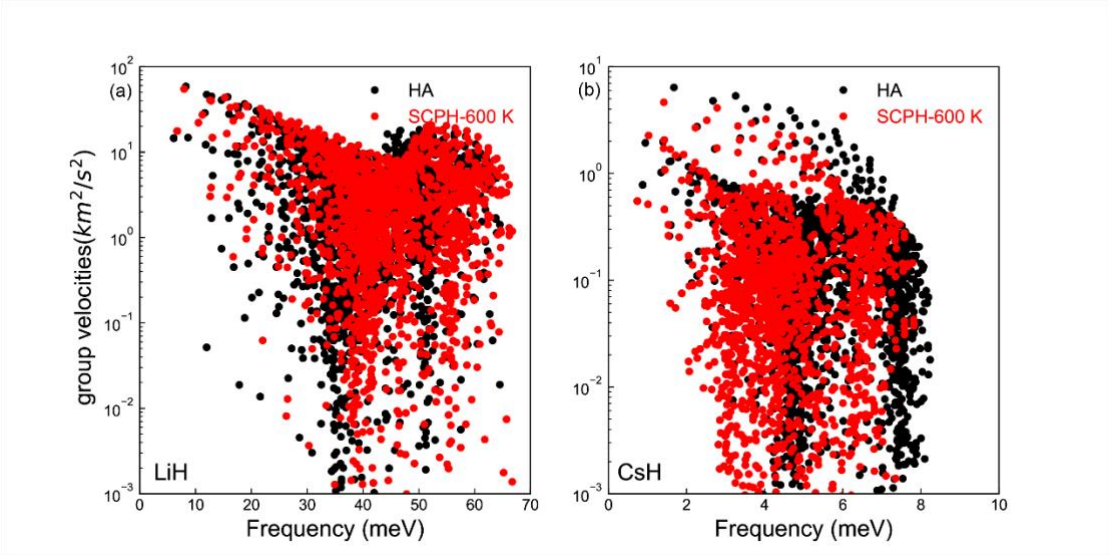

Fig. S2 Phonon group velocities for LiH and CsH.

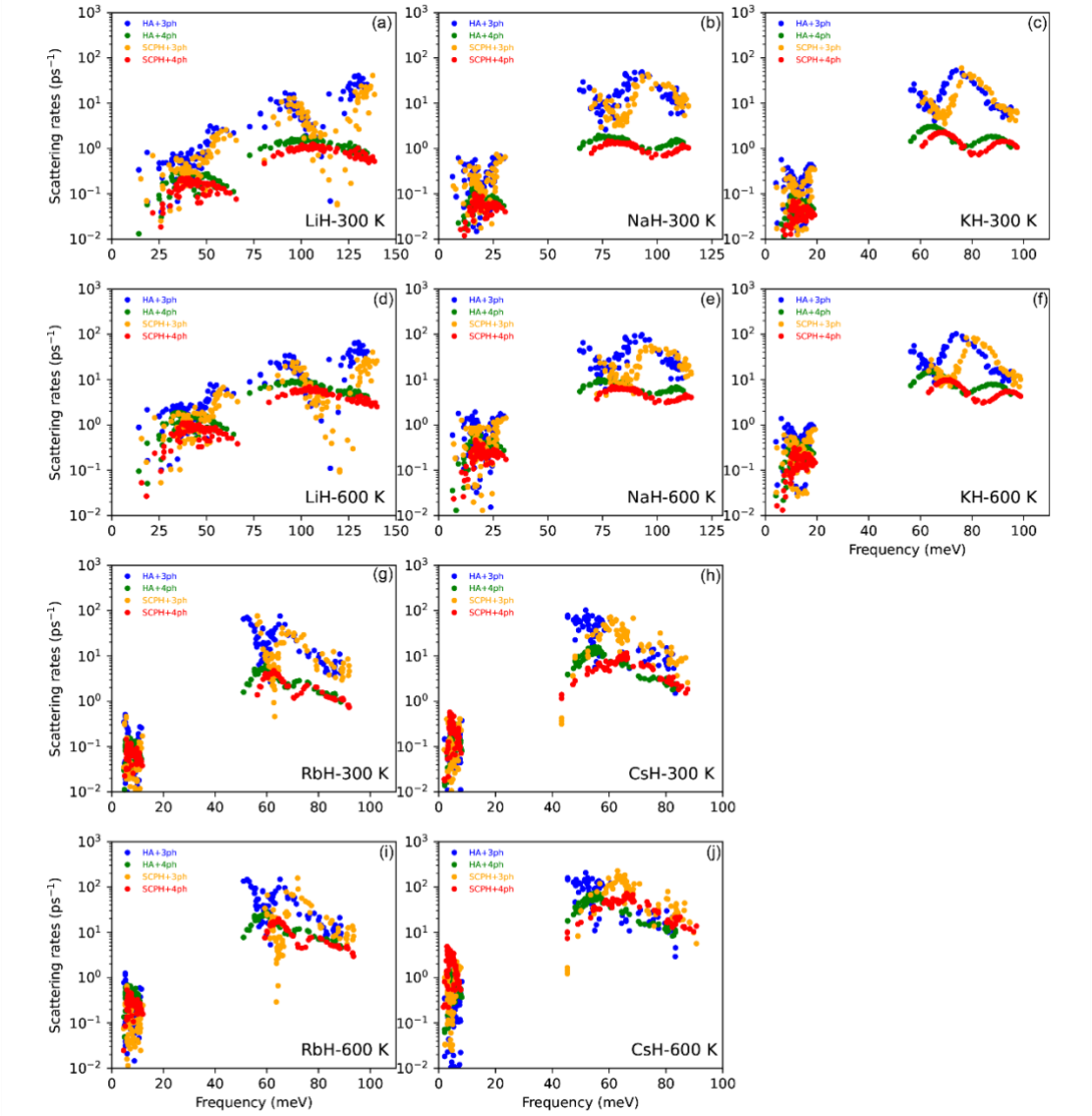

FIG. S3. Phonon scattering rates at 300 K and 600 K for XH materials. The yellow, green, orange, and red circles represent HA+3ph, HA+4ph, SCPH+3ph, and SCPH+4ph, respectively.

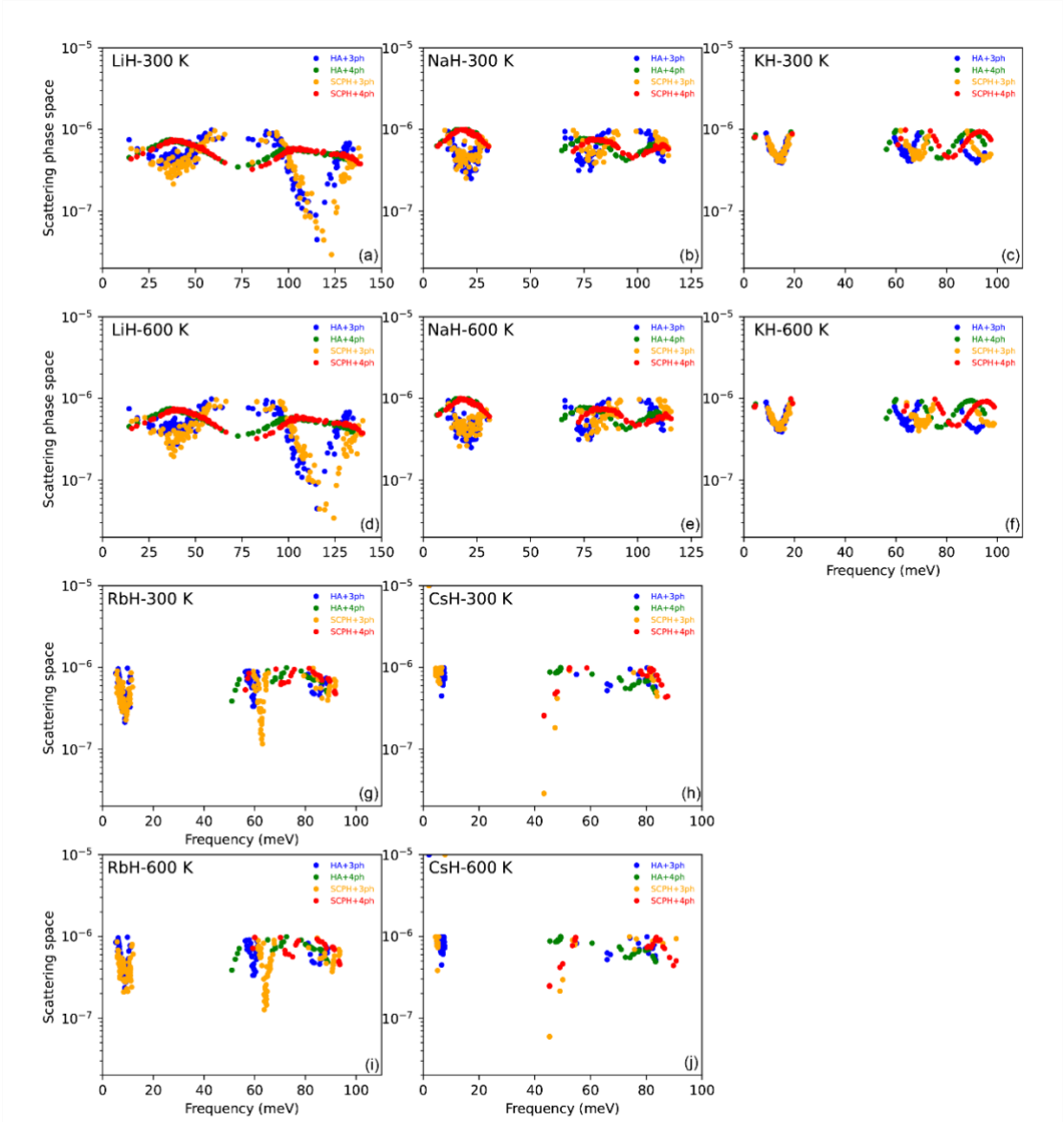

FIG. S4. Phonon scattering phase spaces at 300 K and 600 K for XH materials. The yellow, green, orange, and red circles represent HA+3ph, HA+4ph, SCPH+3ph, and SCPH+4ph, respectively.

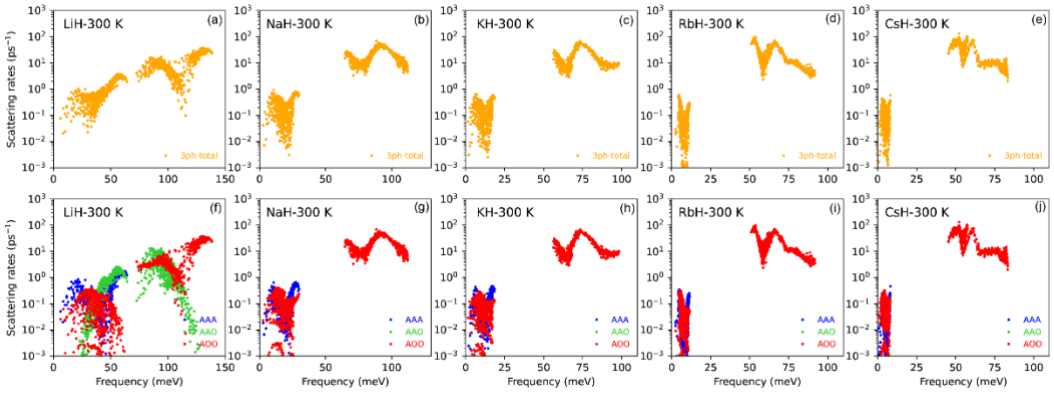

FIG. S5. The total phonon-phonon scattering rates (a-e) and split mode scattering rates (f-j) of 3ph scattering in XH (X= Li, Na, K, Rb, Cs). The orange points represent the total 3ph scattering rates. The blue points, green points, and red points display AAA-type, AAO-type, and AOO-type scatterings, respectively. "A" stands for acoustic and "O" for optical phonons. Each phonon scattering process must simultaneously conserve energy and momentum.

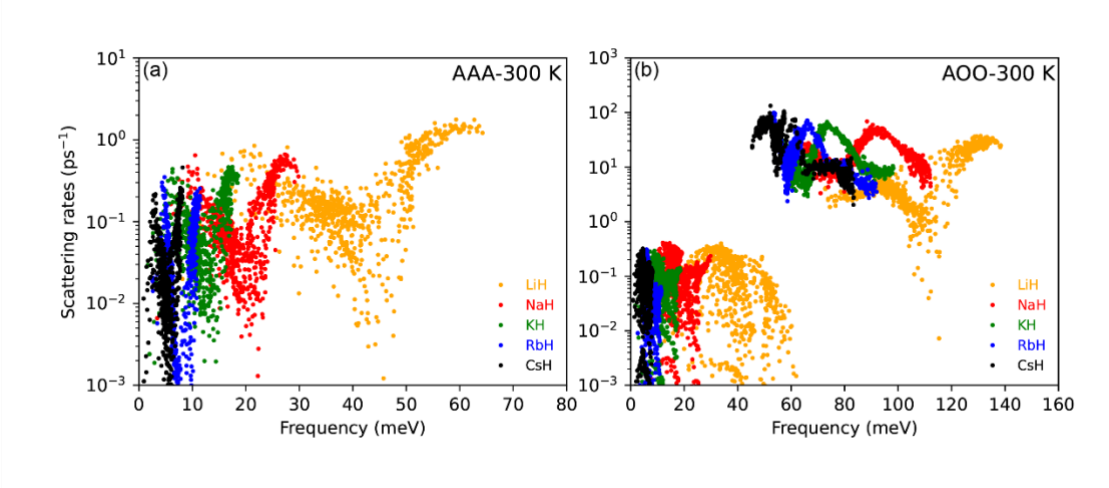

FIG. S6. The AAA-type scattering rates (a) and AOO-type scattering rates (b) of 3ph scattering in XH (X= Li, Na, K, Rb, Cs).

Fig. S5 categorizes the total three-phonon scattering into AAA, AOO, and AAO. It is worth noting that AAO scattering (green points) is absent in the four heavier materials. This absence is due to the significant acoustic optical (A-O) gap resulting from the large atomic mass ratio, which suppresses AAO scattering. In order to see the scattering change more clearly, we separate AAA scattering and AOO scattering in Fig. S6. We observe the decrease in AAA scattering as the atomic mass of the heavier atom increases. This decrease is a consequence of lower acoustic branch frequencies and acoustic phonon bunching. The thermal conductivity is mainly contributed by the acoustic phonon. So we only focus on the low-frequency part of AOO scattering. At low frequencies, AOO scattering decreases with increasing atomic mass.

For LiH, we find some experimental and theoretical data about its lattice thermal conductivity. We compare in the Table. SII. Our results are close to the previous theoretical ones. The gap between experimental data and our results is because of the impure

polycrystalline samples which will further induce the phonon-boundary scattering and finally decrease the lattice thermal conductivity. Besides, we also do not consider thermal expansion. Except for LiH, we did not find any more experimental data for the other materials.

T (K)	Exp ($Wm^{-1}K^{-1}$)	Theo ($Wm^{-1}K^{-1}$)	Our ($Wm^{-1}K^{-1}$)
300	12.47 [3] 14.7[4]	23.00 [3],18.3[4]	19.7
600	6.24[3]	9.35[3]	8.22

Table. SII Compare the lattice thermal conductivity of LiH.

In Table. SIII, we use the phase space ratio of P_4/P_3 as an intuitive expression to measure the variation of the scattering phase space [5]. Our calculation shows that the ratio of P4/P3 increases as the atomic mass ratio increases, except for CsH, which is consistent with Fig. 3(a).

T	LiH	NaH	KH	RbH	CsH
100 K	1.20	1.22	1.78	2.03	1.26
200 K	1.20	1.22	1.78	2.03	1.26
300 K	1.20	1.22	1.78	2.03	1.26
400 K	1.20	1.22	1.78	2.03	1.26
500 K	1.20	1.22	1.78	2.03	1.26
600 K	1.20	1.22	1.78	2.03	1.26
700 K	1.20	1.22	1.78	2.03	—
800 K	1.20	122	1.78	2.03	—
900 K	1.20	1.22	1.78	2.03	—

Table.SIII. P4/P3 for $\kappa_{3,4ph}^{HA}/\kappa_{3ph}^{HA}$. P4 represents 4ph scattering phase space for $\kappa_{3,4ph}^{HA}$. P3 represents 3ph scattering phase space for κ_{3ph}^{HA} .

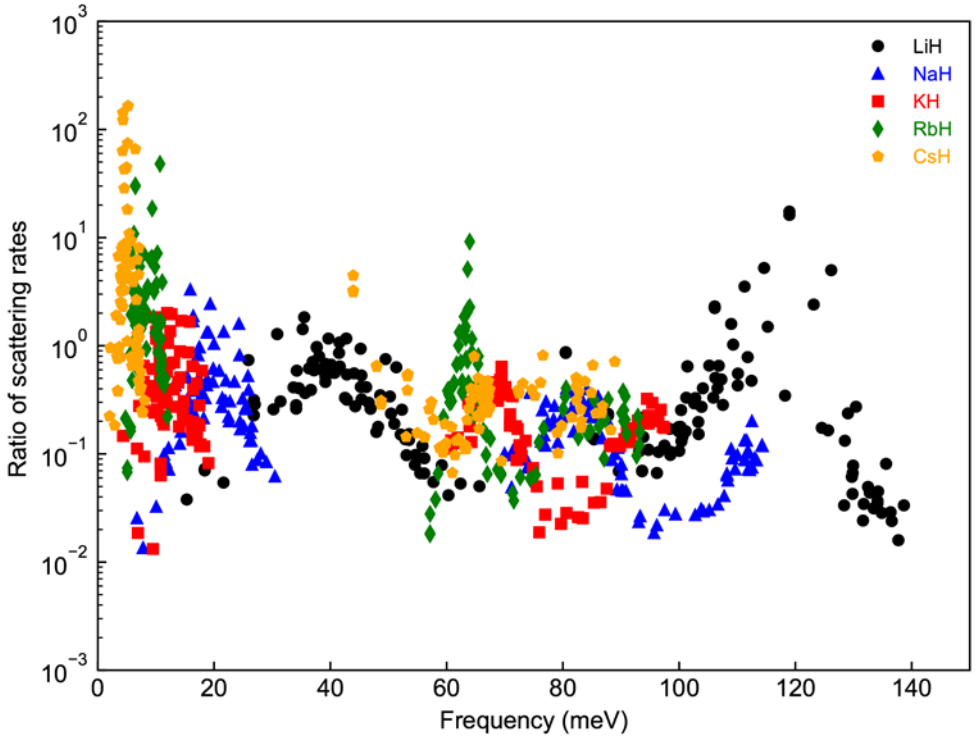

FIG. S7. The ratio of phonon scattering rates (α_4/α_3) for XH materials $\alpha_4 = 1/\tau_4$ and $\alpha_3 = 1/\tau_3$ at the whole phonon frequency range.

Thermal conductivity (LiH) (W m^{-1} K^{-1})	3ph	4ph	3ph+SCPH	4ph+SCPH
300 K	24.3	19	34	25.6
600 K	11.2	6.78	18.3	12
300 K+QHA	18.8	15.9	26..4	20.8
600 K+QHA	7.4	4	27.3	15.7

Table. SIV The lattice thermal conductivity of LiH with thermal expansion.

References:

1. Jiongzhi Zheng, Dongliang Shi, Yuewang Yang, Chongjia Lin, He Huang, Ruiqiang Guo, and Baoling Huang, Anharmonicity-induced phonon hardening and phonon transport enhancement in crystalline perovskite $BaZrO_3$, *Phys. Rev. B* **105,** 224303 (2022).

2. Gang Liu, Zhibin Gao, Jian Zhou, Strain effects on the mechanical properties of Group-V monolayers with buckled honeycomb structures, *Physica E-Low-Dimensional Systems & Nanostructures,* **112,** 59-65 (2019).

3. L. Lindsay, Isotope scattering and phonon thermal conductivity in light atom compounds: LiH and LiF, *Phys. Rev. B* **94,** 174304 (2016).

4. Yi Xia, Vinay I. Hegde, Koushik Pal, Xia Hua, Dale Gaines, Shane Patel, Jiangang He, Muratahan Aykol, and Chris Wolverton, High-Throughput Study of Lattice Thermal Conductivity in Binary Rocksalt and Zinc Blende Compounds Including Higher-Order Anharmonicity, *Phys. Rev. X* **10,** 041029 (2020).

5. Hezhu Shao, Daquan Ding, Ying Fang, Wei Song, Jielan Huang, Changkun Dong, and Hao Zhang, Phonon transport in Cu_2GeSe_3: Effects of spin-orbit coupling and higher-order phonon-phonon scattering, *Phys. Rev. B* **107,** 085202 (2023).